Available online at www.sciencedirect.com

ScienceDirect

Journal of Photochemistry and Photobiology A: Chemistry 191 (2007) 74–79

Journal of Photochemistry and Photobiology A:Chemistry

www.elsevier.com/locate/jphotochem

# Novel luminescent lanthanide complexes covalently linked to a terpyridine-functionalized silica network

Bi-Hai Tong, Shuan-Jin Wang, Jian Jiao, Fu-Ri Ling, Yue-Zhong Meng, Biao Wang *

*State Key Laboratory of Optoelectronic Materials and Technologies, Institute of Optoelectronic and Functional Composite Materials, Sun Yat-Sen University, Guangzhou 510275, PR China*

Received 25 December 2006; received in revised form 21 March 2007; accepted 5 April 2007

Available online 8 April 2007

## Abstract

Novel luminescent organic–inorganic hybrid materials consisting of lanthanide ($Eu^{3+}$, $Tb^{3+}$) complexes covalently bonded to a silica-based network have been obtained by a sol–gel approach. A new monomer has been synthesized by the thiol-ene photopolymerization between γ-mercaptopropyltrimethoxysilane and 4′-allyloxy-2,2′:6′,2″-terpyridine. The monomer is afterward submitted to complexation with lanthanide ions and used as the siloxane network precursor. FT-IR, DR, SEM, luminescence spectra and decay analysis, as well as luminescence quantum yields, were used to characterize the obtained hybrid materials. Excitation at the ligand absorption wavelength (333 nm) resulted in strong emission of the lanthanide ions: $Eu^{3+}$ $^5D_0$–$^7F_J$ ($J = 0$–4) and $Tb^{3+}$ $^5D_4$–$^7F_J$ ($J = 6, 5, 4, 3$) emission lines due to efficient energy transfer from the ligands to the lanthanide ions. When the $Eu^{3+}$ and $Tb^{3+}$ ions were incorporated into the same hybrid material, only the simple addition spectra from the two metal centers was observed, which indicated bimetallic complex was not formed.

© 2007 Published by Elsevier B.V.

*Keywords:* Terpyridine; Lanthanides; Luminescence; Thiol-ene photopolymerization; Organic–inorganic hybrid materials

## 1. Introduction

The lanthanide ions are well-known for their photoluminescence properties in the visible and near-infrared regions [1]. The importance of lanthanide ions is related to the particularities of their luminescence, that is, long decay times and narrow-band emission. Unfortunately, since the f–f* transitions of lanthanide ions are forbidden by the Laporte rule, they absorb little excitation energy in the visible and UV regions. Organic ligands are known to be efficient sensitizers for the luminescence of lanthanide ions. The formation of complex between a lanthanide ion and a certain organic ligand has a double beneficial effect on both protecting metal ions from vibrational coupling and increasing the light absorption cross section by “antenna effects” [2,3]. However, the practical use of these complexes as luminescent devices or tunable solid-state lasers has not been realized because of their poor photo and thermal stability and mechanical properties [4].

Recently, there has been considerable interest in the optical properties of luminescent species in sol–gel derived siloxane hybrid materials for photonic applications due to the fact that they potentially combine the optical quality of silica, its thermal stability and its mechanical strength together with the optical characteristics of active species [5–9]. Good control of the coupling between the hosts and the guest molecules has been quite useful for the design of hybrid materials for definite applications. Typically, these materials were obtained by doping silica gel with the lanthanide complexes or organic dyes (class I hybrid materials) [10–15], where only weak interactions exist between the organic and inorganic parts. Consequently, the clustering of emitting species is difficult to prevent by this method. Inhomogeneous dispersion of both components and leaching of dopants are observed in class I hybrid materials for which the concentration of organic species is also limited.

In this study, covalent grafting of the ligand to the silica backbone via Si–C bonds will allow us to overcome these drawbacks. The as-derived class II hybrid materials were monophasic even at a high concentration of organic ligands, and the reinforcement of thermal and mechanical resistances has been clearly established [16–24].

---

* Corresponding author. Tel.: +86 20 84115692; fax: +86 20 84115692.
*E-mail address:* wangbiao@mail.sysu.edu.cn (B. Wang).

1010-6030/$ – see front matter © 2007 Published by Elsevier B.V.
doi:10.1016/j.jphotochem.2007.04.005

Terpyridines are among the *N*-heterocycles that have very high binding affinity towards various cations which are attractive features for the construction of tunable chromophores [25–27]. Indeed, terpyridines can form complexes with lanthanide ions such as $Eu^{3+}$ and $Tb^{3+}$. In such cases, the terpyridine ligand absorbs exciting near–UV radiations and channel it to the lanthanide ions.

In this paper, a new kind of compound (denoted TERPY–Si) containing terpyridine that plays a double role, i.e., as a ligand of the lanthanide ions and as a precursor of the sol–gel process, was synthesized conveniently by thiol-ene photopolymerization. The luminescent hybrid materials were prepared by hydrolysis and co-condensation of tetraethoxysilane (TEOS) and TERPY–Si in the presence of $Eu^{3+}$ (or $Tb^{3+}$). The silica hybrid was synthesized without the addition of any acidic or basic catalysis to avoid decomposition and protonation of the terpyridine group. The transparent monolithic gels were studied by scanning electron microscopy (SEM). Luminescence spectra of the lanthanide complexes were recorded, and the luminescence lifetimes were measured.

## 2. Experimental

### 2.1. Chemicals and procedures

γ-Mercaptopropyltrimethoxysilane (MPS, 95.8%) was purchased from Nanjing Shuguang Chemistry plant. The solvent acetonitrile was dried with calcium hydride and redistilled. Europium and terbium nitrates were obtained from the corresponding oxides $Eu_2O_3$ (99.99%) and $Tb_4O_7$ (99.99%). 4′-Allyloxy-2,2′:6′,2″-terpyridine (ATP) was synthesized according to Ref. [28]. The procedure for the preparation of TERPY–Si was according to reaction scheme in Fig. 1.

TERPY–Si was prepared as follows: a mixture of MPS (0.35 g, 1.7 mmol), ATP (0.50 g, 1.7 mmol), and acetonitrile (15 mL) were degassed and sealed under nitrogen. Then the solution was exposed to UV illumination using a 100 W high pressure mercury lamp with primary output at 365 nm. After 20 min, the solvent was removed in vacuo and the pasty residue was washed with cold hexane, then a clear oil of TERPY–Si was obtained.

$^1H$ NMR (DMSO): $\delta$ 8.71 (2H, $H_6$ and $H_{6''}$), 8.60 (2H, $H_3$ and $H_{3''}$), 7.98 (4H, $H_{3'}$ $H_{5'}$ $H_4$ and $H_{4''}$), 7.49 (2H, $H_5$ and $H_{5''}$), 4.33 (2H, $H_7$), 3.45 (9H, $H_{13}$), 3.27 (2H, $H_9$), 2.69 (2H, $H_{10}$), 2.08 (2H, $H_8$), 1.59 (2H, $H_{11}$), 0.70 (2H, $H_{12}$); $^{13}C$ NMR (DMSO): $\delta$ 166.4 ($C_{4'}$), 156.4 ($C_{2'}$ and $C_{6'}$), 154.7 ($C_2$ and $C_{2''}$), 148.9 ($C_2$ and $C_{2''}$), 137.0 ($C_4$ and $C_{4''}$), 124.1 ($C_3$ and $C_{3''}$), 120.6 ($C_5$ and $C_{5''}$), 106.5 ($C_7$), 66.3 ($C_{13}$), 49.8 ($C_4$), 33.8 ($C_{10}$), 28.5 ($C_9$), 27.2 ($C_8$), 22.5 ($C_{11}$), 7.8 ($C_{12}$). MS(EI) *m*/*e* = 486.0 ($M^+$).

The hybrid materials were prepared as follows: TERPY–Si (0.50 g, 1.0 mmol) was dissolved in 2 mL of *N*,*N*′-dimethylformide (DMF), TEOS and $H_2O$ were added to it with the molar ratio 1:4:16 (TERPY–Si:TEOS:$H_2O$) under stirring. The $Eu(NO_3)_3$($Tb(NO_3)_3$) solution of DMF was added to the resulting mixture, the ratio of TERPY–Si to lanthanide ions being 1:1. The mixture was agitated magnetically to achieve a single phase and then transferred into a cuvette. Thermal curing was performed at 60 °C and continued until the sample solidified. After 5 days, the samples were dried for 24 h at 100 °C and collected as monolithic bulks and ground as powder materials for the photophysical studies.

### 2.2. Measurements

All measurements completed under room temperature. $^1H$ NMR and $^{13}C$ NMR spectra was recorded on a Bruker Avance 400 spectrometer with tetramethylsilane (TMS) as internal reference. Mass spectra were taken on a Thermo DSQ low resolution mass spectrometer. The steady-state luminescence spectra and the lifetime measurements were measured on an Edinburgh

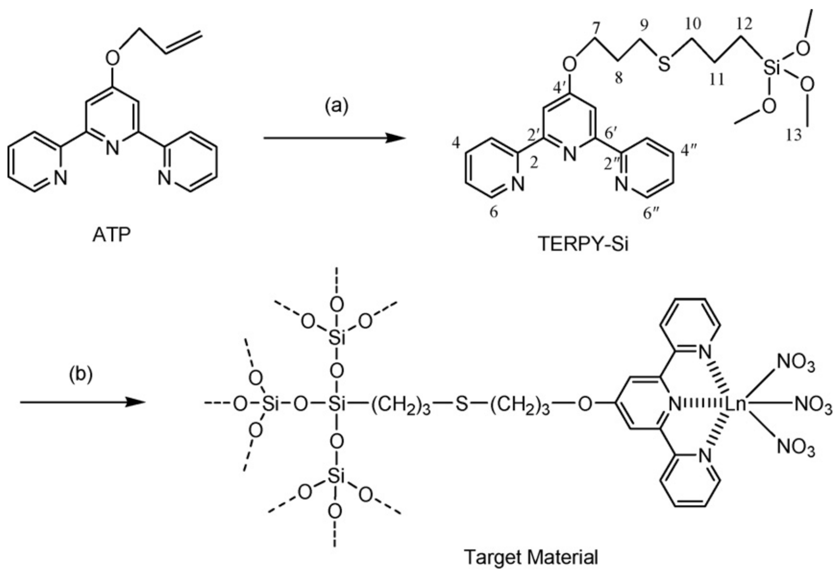

Fig. 1. Scheme of the synthesis process of TERPY–Si and predicted structure of hybrid materials. Reagents and experimental conditions: (a) MPS, $CH_3CN$, UV, 20 min; (b) $Eu(NO_3)_3\cdot 6H_2O$ or $Tb(NO_3)_3\cdot 6H_2O$, TMOS, $H_2O$, DMF.

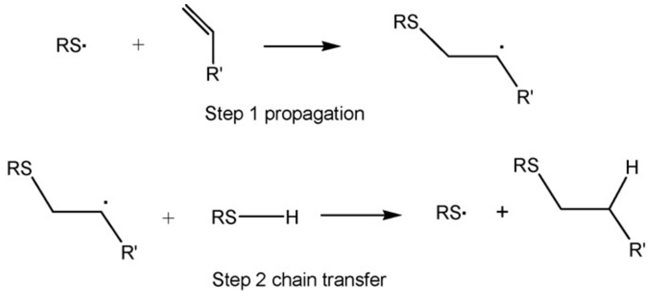

Fig. 2. Scheme of the thiol-ene photopolymerizations.

Instruments FLS 920 spectrometer. Scanning electron microscope (SEM) images were obtained with a JEOL JSM-6330F. IR spectra were measured on a Perkin-Elmer spectrum 100 spectrophotometer using KBr pellets. The diffuse reflectance (DR) measurements were performed on an UV-2501PC spectrophotometer. The luminescence quantum yields were tested similarly to Greenham's way [29] in an integrating sphere (IS-80, Lab-Sphere Co.) under an excitation of 325 nm.

## 3. Results and discussion

Thiol-ene photopolymerizations are based on the addition of a thiol to a vinyl(ene) functional group [30]. The addition, as outlined in Fig. 2 involves propagation of a thiyl radical through a vinyl functional group (step 1), followed by chain transfer to another thiol functional group (step 2). Almost quantitative conversion can be obtained by UV irradiation without any added photoinitiator [31]. In addition, the reactions not produce small molecules (such as HCl). These properties facilitate the preparation of organotrialkoxysilane derivatives which are sensitive to moisture.

Fig. 3 displays the IR spectra of ATP (a), TERPY–Si (b), TERPY–Si–Eu (c) and TERPY–Si–Tb (d). In Fig. 3b, no absorption band located at approximately 1649 cm$^{-1}$ assigned to the vibration of the $CH_2CH{=}CH_2$ group can be observed, indicating the completion of grafting reactions. The $\nu$Si–OMe absorption bands located near 1029 cm$^{-1}$. In Fig. 3c and 3d, the broad absorption band at 1063–1013 cm$^{-1}$ ($\nu$Si–O–Si) indicates the formation of siloxane bonds. The $\nu$Si–C vibration located in the 1163 cm$^{-1}$ wavelength is observed which is consistent with the fact that no Si–C bond cleavage occurs during hydrolysis/condensation reactions.

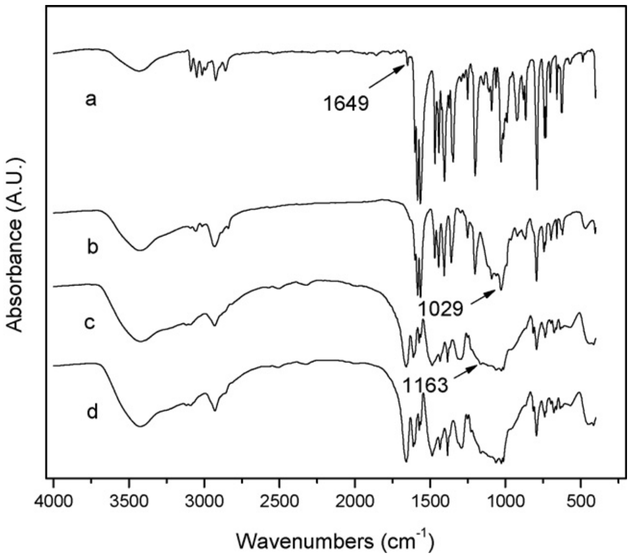

Fig. 3. FT-IR spectra for ATP (a), TERPY–Si (b), TERPY–Si–Eu (c) and TERPY–Si–Tb (d).

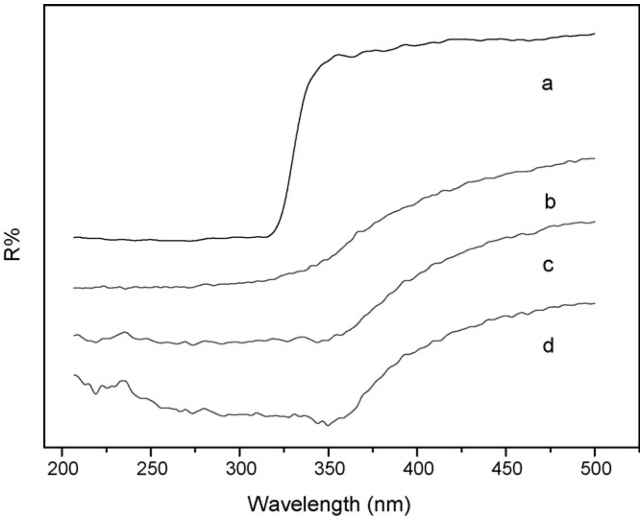

Fig. 4. DR spectra of ATP (a), TERPY–Si (b), TERPY–Si–Eu (c) and TERPY–Si–Tb (d).

The DR spectra of the ATP (a), TERPY–Si (b), TERPY–Si–Eu (c) and TERPY–Si–Tb (d) are shown in Fig. 4. In the UV region of curves a–d (200–400 nm) broad absorption bands are both observed and can be attributed to electronic transitions from the ground-state level ($\pi$) $S_0$ to the excited level ($\pi^*$) $S_1$ of the organic ligands. Comparing (b) with (a), we can see a red shift and the change of curve shape after thiol-ene photopolymerization because the $-SCH_2CH_2CH_2Si(OCH_3)$ group has absorption in the longer wavelength region.

The scanning electron micrographs (Fig. 5) for TERPY–Si hybrid materials show that homogeneous materials were obtained and no phase separation was observed, but many large pore-like holes were also observed in terms of the backbone leaving behind by the result of hydrolysis and polycondensation of silica hosts. Because of the strong covalent bonds bridging between the inorganic and organic phases, they are composed rather uniformly so that the two phases can exhibit their distinct properties together.

The excitation spectra of TERPY–Si–Eu and TERPY–Si–Tb are shown in Fig. 6 (Ex) and Fig. 7 (Ex), respectively. These spectra were obtained by monitoring the emission of the Eu$^{3+}$ ions at 618 nm and Tb$^{3+}$ at 544 nm. For TERPY–Si–Eu, the excitation spectrum is dominated by a broad band centered at 333 nm, which is the characteristic absorption of the lanthanide complexes arising from the efficient transition based of the conjugated double bonds of the heterocyclic ligand. So was TERPY–Si–Tb (333 nm).

All emission spectra were obtained by excitation at 333 nm. As can be seen from Fig. 6A, the emission band (Fig. 6B)

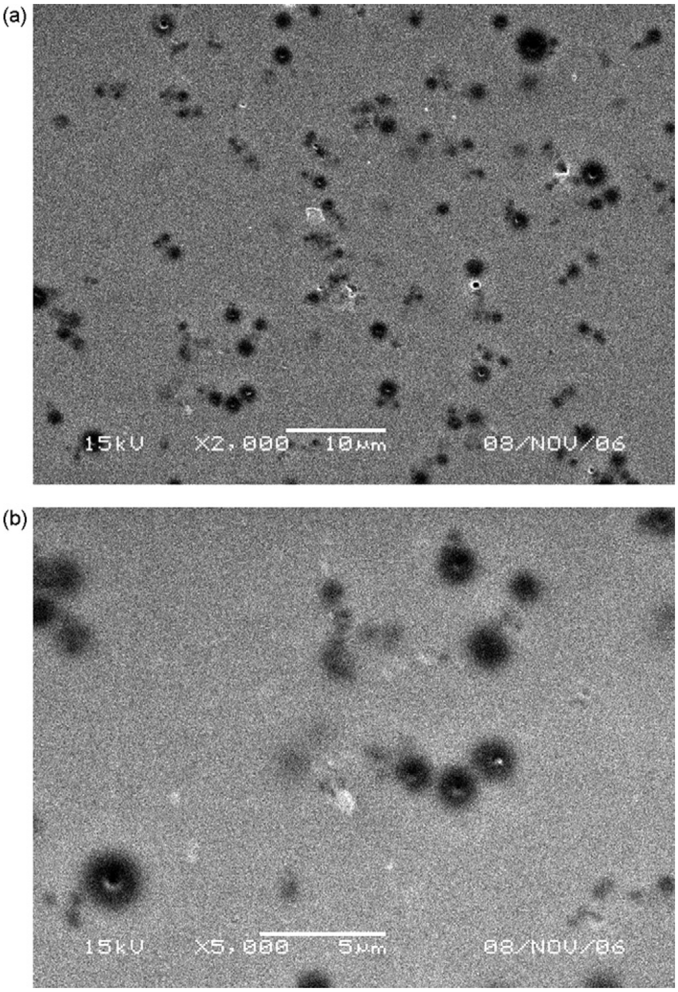

Fig. 5. Scanning electron micrographs for TERPY–Si–Eu (a) and TERPY–Si–Tb (b). Prior to the test, the surface was sputtered with platinum for 100 s.

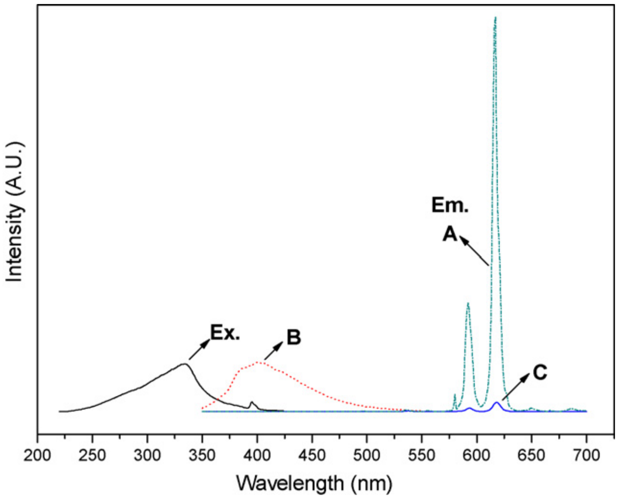

Fig. 6. Excitation spectrum of TERPY–Si–Eu (Ex) and emission spectra of TERPY–Si–Eu (A), TERPY–Si (B), and $Eu(NO_3)_3$ (C).

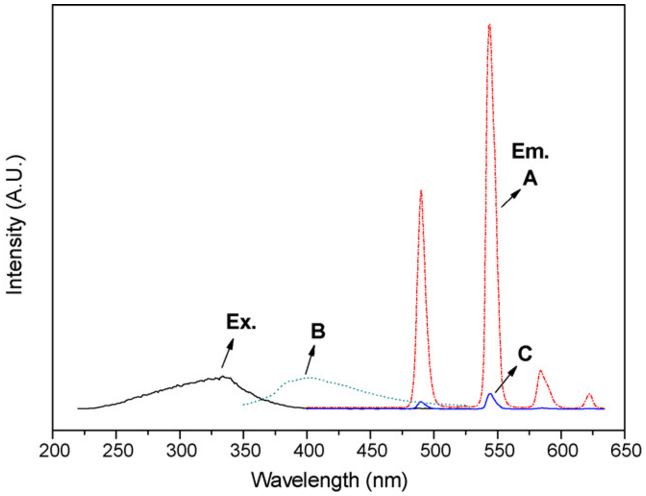

Fig. 7. Excitation spectrum of TERPY–Si–Tb (Ex) and emission spectra of TERPY–Si–Tb (A), TERPY–Si (B), and $Tb(NO_3)_3$ (C).

of TERPY–Si centered at 368 nm is disappeared while the characteristic peaks of $Eu^{3+}$ ($^5D_0$–$^7F_J$ ($J = 0$–4)) are prominently strengthened compared with that of $Eu(NO_3)$ (Fig. 6C). This indicates that energy transfer could take place from the terpyridine group to the lanthanide ion, that is, coordination occurs. The $^5D_0$–$^7F_1$ transition is independent of the environment but the $^5D_0$–$^7F_2$ is hypersensitive [32]. The intensity ratio $I(^5D_0–^7F_2)/I(^5D_0–^7F_1)$ of $Eu(NO_3)_3$ (2.7) was smaller than that of TERPY–Si–Eu (3.5), indicating the coordination leads to a increase in the odd parity (asymmetry) of Eu(III) complexes [33]. The homogeneity of TERPY–Si–Eu is shown well in Fig. 6A, which displays only one line for the $^5D_0$–$^7F_0$ emission. As far as the emission spectrum of TERPY–Si–Tb is concerned, four lines of $Tb^{3+}$ $^5D_4$–$^7F_J$ ($J = 3$–6) emission can be detected in the visible spectrum. The most prominent line is observed at approximately 544 nm, which has a increased branching ratio (from 0.58 to 0.62) after coordination. From the spectra, it was observed that the resulting hybrid materials possessed excellent luminescence characteristics, not only strong emission intensity but also narrow half emission width (12 nm for TERPY–Si–Eu and 8 nm for TERPY–Si–Tb).

Tew and co-worker [34] recently reported a novel yellow emission and thermochromism in the lanthanide–terpyridine-based polymeric alloys containing $Eu^{3+}$ and $Tb^{3+}$. Here, these two different lanthanide ions were also incorporated into the same hybrid material to study the luminescence behavior. The emission curve for this sample (TERPY–Si–Eu–Tb) reported in Fig. 8. Only the simple addition spectra from the two metal centers was observed. This results can be explained by the concept of site isolation [35], i.e., specific entities can be considered as the binding sites for metal ions. Here, the monomer plays a double role, that is, as a precursor for the sol–gel and as the binding site for the lanthanide ions, confining the migration of the lanthanide ions and the aggregation to large particles. Upon hydrolysis and condensation, the ligands form a preliminary network, which further restricts approach of the lanthanide ions.

Fig. 9 presents the typical decay curves of the hybrid materials. Both of the decay curves can be well-fitted by a single

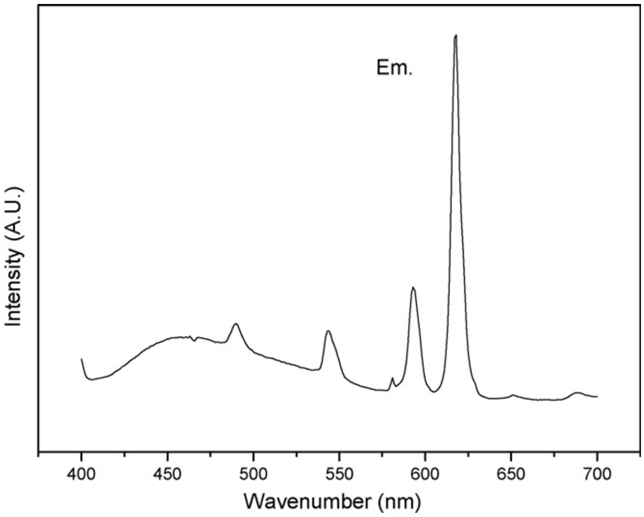

Fig. 8. Emission spectra of the 1:1 europium(III)/terbium(III)-co-doped hybrid material (TERPY–Si–Eu–Tb) excited at 333 nm.

exponential function: $I = I_0 + A\exp[-(t-t_0)/\tau]$ ($A$ is the constant, $I_0$ the intensity at $t_0$, and $\tau$ is the lifetime) confirming that all $Ln^{3+}$ ions lie in the same average environment. The luminescence lifetimes were determined to be 1.0 ms for $Eu^{3+}$ ions and 0.8 ms for $Tb^{3+}$ ions by the above fits. In general, the radiative lifetime of the $^5D_0$ state of $Eu^{3+}$ ions falls in the millisecond range [36,37], the experimental decay time is in this range, indicating that the ligand used are efficiently shielding $Ln^{3+}$ ions from their surroundings.

The emission quantum yield of TERPY–Si–Eu was 34% and that of TERPY–Si–Tb was 75%. The results indicated that the quenching by high-energy vibrations (O–H, C–H) and concentration was not severe. The emission quantum yield of TERPY–Si–Tb was much larger than that of TERPY–Si–Eu. Efficient energy transfer from terpyridine moiety to the terbium(III) ion compared to the europium(III) ion probably caused by the energy matching of the triplet level.

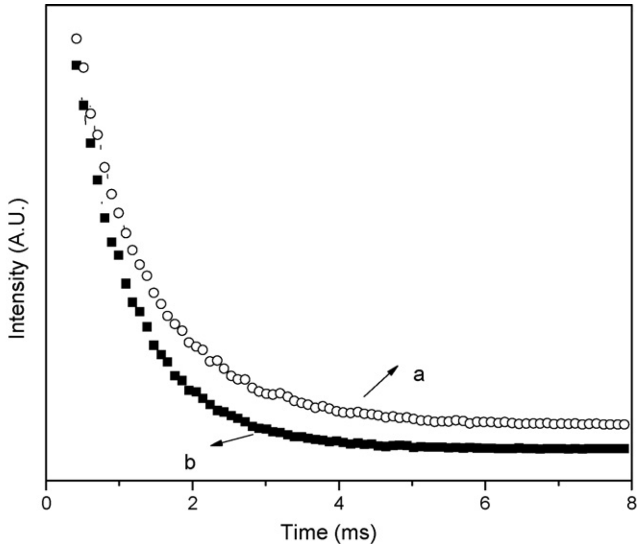

Fig. 9. $^5D_0$ decay curve (a) of $Eu^{3+}$ and $^5D_0$ decay curve (b) of $Tb^{3+}$ excited at 333 nm in hybrid materials TERPY–Si–Eu and TERPY–Si–Tb.

## 4. Conclusions

A kind of compound for sol–gel containing terpyridine, which plays a double role, i.e., as a ligand for lanthanide ions and as a precursor for sol–gel has been synthesized and characterized. Novel hybrid materials covalently linked with lanthanide complexes have been prepared and characterized in detail. There is no obvious phase separation in these hybrid materials and the lanthanide complexes can be doped in these hybrid monoliths uniformly. The final hybrids show strong, characteristic emissions of $Eu^{3+}$ and $Tb^{3+}$ ions by intramolecular energy transfer from the triplet state energy of terpyridine group to the resonant emissive energy level of the central $Ln^{3+}$. There is predominantly one type of $Ln^{3+}$ binding site with the materials.

Hence, it is anticipated that this homogeneous hybrid materials with strong covalent bonds will attract interest for its utilization in optical or electronic applications.

## Acknowledgments

This work was supported by the National Natural Science Foundation (nos. 10572155, 10172030 and 50232030), Canton Province Sci & Tech Bureau (Key Strategic project Grant Nos. A1100402, A10704004 and A50102004).

## References

[1] J.Y. Li, The Application of Rare-earth Luminescence Materials, Chemical Industry Press, BeiJing, 2003.
[2] N. Sabbatini, M. Guardingli, J.M. Lehn, Coord. Chem. Rev. 123 (1993) 201–228.
[3] N. Sabbatini, A. Mecati, M. Guardigli, J. Lumin. 48 (1991) 463–468.
[4] Q.M. Wang, B. Yan, Inorg. Chem. Commun. 7 (2004) 747–750.
[5] M. Casalboni, F. De Matteis, V. Merio, Appl. Phys. Lett. 83 (2003) 416–418.
[6] M.R. Kim, Y.L. Choi, S.W. Park, Dyes Pigm. 70 (2006) 171–176.
[7] S. Kucharski, R. Janik, Opt. Mater. 27 (2005) 1637–1641.
[8] I.G. Marino, D. Bersani, P.P. Lottici, Opt. Mater. 15 (2001) 279–284.
[9] J.L.H. Jiwan, E. Robert, J.P. Soumillion, J. Photochem. Phtobiol. A 122 (1999) 61–68.
[10] L.N. Sun, H.J. Zhang, J. Phys. Chem. B 109 (2005) 6174–6182.
[11] L.N. Sun, H.J. Zhang, Adv. Funct. Mater. 15 (2005) 1041–1048.
[12] F.J. Rodriguez, C. Sanchez, B. Villacampa, Opt. Mater. 28 (2006) 480–487.
[13] A. Costela, I. Garcia Moreno, Chem. Phys. Lett. 387 (2004) 496–501.
[14] Y. Yang, G.D. Qian, D.L. Su, Opt. Commun. 239 (2004) 415–420.
[15] A. Anedda, C.M. Carbonaro, F. Clemente, J. Non-cryst. Solids 351 (2005) 1850–1854.
[16] A.C. Franville, D. Zambon, Chem. Mater. 12 (2000) 428–435.
[17] F. Embert, A. Mehdi, C. Reye, R.J.P. Corriu, Chem. Mater. 13 (2001) 4542–4549.
[18] H.R. Li, J. Lin, H.J. Zhang, Chem. Mater. 14 (2002) 3651–3655.
[19] Q.M. Wang, B. Yan, J. Mater. Chem. 14 (2004) 2450–2454.
[20] Q.M. Wang, B. Yan, J. Photochem. Phtobiol. A 175 (2005) 159–164.
[21] P. Lenaerts, A. Storms, Chem. Mater. 17 (2005) 5194–5201.
[22] P. Lenaerts, E. Ryckebosch, J. Lumin. 114 (2005) 77–84.
[23] P. Lenaerts, K. Binnemans, J. Lumin. 117 (2006) 163–169.
[24] Y.L. Sui, B. Yan, J. Photochem. Phtobiol. A 182 (2006) 1–6.
[25] J.P. Sauvage, J.P. Collin, J.C. Chambron, Chem. Rev. 94 (1994) 993–1019.
[26] H. Hofmeier, U.S. Schubert, Chem. Soc. Rev. 33 (2004) 373–399.
[27] P.R. Andres, U.S. Schubert, Adv. Mater. 16 (2004) 1043–1068.
[28] P.R. Andres, H. Hofmeier, U.S. Schubert, Synthesis 18 (2003) 2865–2871.
[29] N.C. Greenham, I.D.W. Samuel, G.R. Hayes, R.T. Phillips, Y.A.R.R. Kessener, Chem. Phys. Lett. 241 (1995) 89–96.

[30] C.E. Hoyle, T.Y. Lee, J. Polym. Sci. A: Polym. Chem. 42 (2004) 5301–5338.

[31] N.B. Cramer, S.K. Reddy, J. Polym. Sci. A: Polym. Chem. 42 (2004) 1752–1757.

[32] M.H.V. Werts, R.T.F. Jukes, J.W. Verhoeven, Phys. Chem. Chem. Phys. 4 (2002) 1542–1548.

[33] Y. Hasegawa, M. Yamamuro, Y. Wada, J. Phys. Chem. A 107 (2003) 1697–1702.

[34] R. Shumugan, G.N. Tew, J. Am. Chem. Soc. 127 (2005) 13567–13572.

[35] M. Nandi, J.A. Conklin, A. Sen, Chem. Mater. 3 (1991) 201–206.

[36] M. Buijs, A. Meijering, G. Blasse, J. Lumin. 37 (1987) 9–20.

[37] H.R. Li, J.B. Yu, F.Y. Liu, N. J. Chem. 28 (2004) 1137–1141.